NTNU – Trondheim
Norwegian University of
Science and Technology

Statistics of Electric Power Blackouts: Data Analysis and Data Modeling

Friew Gebremedhin-Abraha

Condensed Matter Physics
Submission date: August 2013
Supervisor: Alex Hansen, IFY

Norwegian University of Science and Technology
Department of Physics

”This study is dedicated to God and to my self”

Abstract

Power grids are the most prominent infrastructure due to the fact that the daily life of modern society is directly or indirectly integrated to electric power consumption. And when it is exposed to failures due to human or natural factors, detecting and repairing failed component of the system can initiate another failures. Hence, modelling and analysing failure could help understanding of characteristics of blackout distribution on the network and predict the impact of the failure on interconnected systems.

The theoretical and statistical analysis of the empirical power blackouts using scaled window variance and rescaled range methods shows that size of failure distribution can be elegantly described by power law. The statistical results obtained by applying both methods are consistent. Because there is a long range time correlation between the successive time series of the blackout events measured by the Hurst coefficient which are greater than half but smaller than one. However, for the North American case, scaled window variance result for Hurst coefficient is approximately one means the time series of blackout events is deterministic.

The results of the square lattice model showed that for a relatively smaller lattice size($L < 80$), the probability density function of the conductance change follows Gaussian distribution independent of the tolerance of the conducting lines. However, for lattice sizes below 180 but greater or equal to 80, the probability density function of the conductance change follows power law depending on both tolerance and lattice size. It reveals that when lattice size increase in the given range, the scaling exponent also increase under constant tolerance. But for fixed lattice size, we found that the conductance change depends on tolerance only up to certain value $\alpha = 3.0$.

The cumulative probability distribution of the empirical blackouts from the Norwegian, North American and Ethiopian power grids also show power law. In all the three cases the distribution described by power law falling of faster for larger value of power loss change(ΔP).

Acknowledgement

First and foremost, I would like to express my deepest gratitude to my supervisor Prof. Alex Hansen for his guidance, wisdom, enthusiasm, and specially for his endless support in dealing with my progress of the master thesis. Working with him helped me opening my eye to the knowledge of complex systems. I able to learn immense experience in my way to finalize the study and I am grateful with the knowledge he provided me as it will help me in my future career.

My thanks also goes to the some workers of Ethiopian dispatch control center for their help in providing blackout data. I am also grateful to my fellow classmates Andreas Liudi Mulyo, Morten Stornes, Andrew dibbs and other friends for their help in fixing software programs and other document set-up which were helpful for my study. Finally, I thank to Nebrom Areaya for his support in proofreading the draft of my study.

Table of Contents

Abstract **i**

acknowledgement **ii**

Table of Contents **iv**

List of Tables **v**

List of Figures **ix**

Abbreviations **ix**

1 Introduction **1**

2 Literature Review **5**

3 The theoretical analysis of blackout **11**

3.1 Autocorrelation 11

3.1.1 Scaled Window Variance(SWV) Method 11

3.1.2 Rescaled range(RSR) methods 15

4 Discussion of Bakke, Hansen and Kertesz model **21**

5 Square lattice model **29**

6 Conclusion **45**

Bibliography **46**

Appendix **51**

List of Tables

3.1 Hurst exponent of blackouts by SWV method 13
3.2 Hurst exponent of blackouts by RSR method. 16

List of Figures

1.1 Basic structure of Electric System[1] 2

3.1 Analysis of Norwegian blackout by using SWV method . . 13
3.2 Analysis of North American blackout by using SWV method 14
3.3 Analysis of Ethiopian blackout by using SWV method . . 15
3.4 Analysis of Norwegian blackout by using RSR method. . . 17
3.5 Analysis of North American blackout by using RSR method. 18
3.6 Analysis of Ethiopian blackout by using RSR method . . . 19

4.1 Probability density function for the conductance lose[2] . . 23
4.2 a)$n(r)$ versus r for exponential and small-world network. b) $P(i)$ versus i. The inset shows ΔG versus i for $\alpha = 3.0$. The solid line in the inset is i^2. [2] 24
4.3 a)cumulative distribution $P(\Delta P)$ for power loss in the Norwegian(373 events) and North American(390 events) power grid. b) $P(\Delta P)\Delta P^{0.65}$ for blackout events ΔP for the Norwegian and North American power grid.[2] 25

5.1 Square lattice network 31
5.2 a) Illustration of 180×180 probability density function of conductance loss for $\alpha = 1.0$ and $\alpha = 3.0$. b) Illustration of 180×180 probability density function of conductance loss for different value of $\alpha = 3.0$ and $\alpha = 6.0$ 32

5.3 a) Illustration of 160×160 probability density function of conductance loss for $\alpha = 1.0$ and $\alpha = 3.0$. b) Illustration of 160×160 probability density function of conductance loss for different $\alpha = 3.0$(blue data points) and $\alpha = 6.0$ . . 33
5.4 a) Illustration of 140×140 probability density function of conductance loss for $\alpha = 1.0$ and $\alpha = 3.0$. b) Illustration of 140×140 probability density function of conductance loss for different values of $\alpha = 3.0$ and $\alpha = 6.0$ 34
5.5 a) Illustration of 120×120 probability density function of conductance loss for $\alpha = 1.0$ and $\alpha = 3.0$. b) Illustration of 120×120 probability density function of conductance loss for different values of $\alpha = 3.0$ and $\alpha = 6.0$ 35
5.6 a) Illustration of 100×100 probability density function of conductance loss for $\alpha = 1.0$ and $\alpha = 3.0$. b) Illustration of 100×100 probability density function of conductance loss for different values of $\alpha = 3.0$ and $\alpha = 6.0$ 36
5.7 a) Illustration of 80×80 probability density function of conductance loss for $\alpha = 1.0$ and $\alpha = 3.0$. b) Illustration of 80×80 probability density function of conductance loss for different values of $\alpha = 3.0$ and $\alpha = 6.0$ 37
5.8 a) Illustration of 60×60 probability density function of conductance loss for $\alpha = 1.0$ and $\alpha = 3.0$. b) Illustration of 60×60 probability density function of conductance loss for different values of $\alpha = 3.0$ and $\alpha = 6.0$ 38
5.9 a) Illustration of 40×40 probability density function of conductance loss for $\alpha = 1.0$ and $\alpha = 3.0$. b) Illustration of 40×40 probability density function of conductance loss for different values of $\alpha = 3.0$ and $\alpha = 6.0$ 39
5.10 a) Illustration of 20×20 probability density function of conductance loss for $\alpha = 1.0$ and $\alpha = 3.0$. b) Illustration of 20×20 probability density function of conductance loss for different values of $\alpha = 3.0$ and $\alpha = 6.0$ 40
5.11 Cummulative distribution $P(\Delta P)$ for blackout events in the American(232events), Norwegian(373 events) and Ethiopian(28 events) 42
5.12 Cummulative distribution $P(\Delta P)$ for blackout events in the American(232events), Norwegian(373 events) and Ethiopian(28 events) 43

Abbreviations

SOC	=	Self-Organized Criticality
PDF	=	Probability Density Function
SWV	=	Scaled Window Variance
RSR	=	Rescaled Range
EEPCO	=	Ethiopian Electric Power Corporation
H	=	Hurst coefficient
X_t	=	Time series of successive events
Y_t	=	Brownian motion of a time series
μ	=	mean
σ	=	standard deviation
τ	=	tau

Chapter 1

Introduction

It is known that power utility is prominent entity for the world to accomplish day to day activities ranging from cooking foods up to running huge and complex industries. Though it was replaced by petroleum from middle of 20th century, coal was the dominant energy supply from late 18th to middle of 20th century through out the world[3]. Due to oil crises since late 20th century, the world turn to ponder on other sources of power. These sources are environmental friendly and cost effective that is renewable source of energy like generating electricity from hydro-power[4].

Human being had some observations of sort of shocks on electric fish[5, 6] dated back from the ancient civilization until it has realized the concept of electric charge or electricity after a careful study has been conducted in 17th century[7]. Following this the science of Electricity and Magnetism becomes a fascinating field of study and inspired researcher for more scientific study. Michael Faraday and later James Clerk Maxwell laid the foundation for the contemporary Science of Electromagnetism for their contribution in discovering electromagnetic induction and its modification[8]. The careful study and realization of physics of Electromagnetism helped to tame from one form of energy to other forms of energy to utilize it for daily life of the world.

Earlier generation distribution systems that are invented in 19th century were inefficient because the power plants or generators had to be placed near the power or load consumer[9](example Edison's early Generator). This invention opened a door for the rapid growth of Ac transmission systems(for example the 11kv Ac line developed by George Westinghouse)

which transmit power over long distance[9].

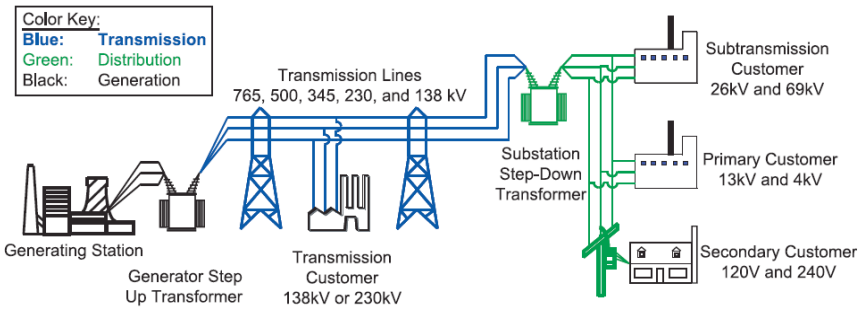

Figure 1.1: Basic structure of Electric System[1]

Today's transmission system is growing into sophisticated and interconnected networks and power plants which operate at different limiting voltages. **Fig.1.1** shows the prototype of topology and features of today's transmission lines. The transmission and distribution of electricity from the power plant or generators to the end user is the aggregate interconnection of lines of networks that deliver about 230v to an ordinary or residential consumers and an intermediate around 12,000v or more to industries or companies[1]. This means the distribution system includes all components from the generation site up to the software operations in the control dispatch. Since the network is sophisticated, it is difficult to analogize and mitigate dynamical and physical phenomena universally when any of these components are exposed to failure. Beside to this, though it is governed by the law of physics, the flow of electricity in the power grid is in all paths available and it is not easily controllable except using control devices(which are more expensive). This together with the fact that electricity flows with very fast speed so that generation and consumption must be simultaneous processes makes failure analysis to be more harder[1].

Despite to it's complexity, researches have been doing exhaustively to investigate mathematical models that better describe the global and dynamical aspects of power grids for optimization purposes. Self-Organized Criticality[10], Cascading model[11], random fuse model[12] and the like are among the models developed and describe that the blackout event exposed in power system exhibits power law. Statistical analysis of the characteristics of dynamical phenomena such as blackout is an input for further study in mitigating, improving and enhancing the components of the power

system.

The main objective of this study is to address the characteristic behaviour of blackout events in Norwegian, North American and Ethiopian power grids. Beside we will discuss squared lattice network model.

The study will provide an overview of the characteristics of the blackout distribution in the three different power systems . The statistical characteristics of the failure distribution which describes the size of the failure will not include quantities such as, energy unversed and restoration time. We will only quantify the size of the failure with power loss during failure. Similarly, the same limitation will be applied to the artificial square lattice. Beside to this, the blackout study in the square lattice model is limited to small lattices size because the processor speed of the computer used to generate data was slow.

The report is warmed up by discussing the introductory part of the the study followed by the literature review to relate previous researches conducted around the area of the study. The third chapter is discussing the theoretical and statistical analysis of blackout for three systems. Following the Bakke and Hansen model, the square lattice model is introduced in chapter five to explain the statistical analysis of the blackout event generated artificially. The last part of the report will include the conclusion of the study and the reference along with the appendix.

Chapter 2

Literature Review

It is not recent history from when human being started to tame natural resources and facilitate their daily life dependently on sophisticated technologies such as electricity, telecommunication, huge industry, digital electronics, computer networks and others. This is because advanced technologies and well functioning infrastructure systems plays extreme importance for every day life, economic prosperity, national security and the like. But unfortunately, components of these technologies can not last longer due to abrupt and inherent(example ageing) factors. Thus, it is inevitable for some failures and disruptions to happen though so many improvements have been doing up to date to minimize the risk or damage due to failure. We can almost certainly agree that the harnessing of electricity can be taken as the most vital technological advances of the contemporary world for prosperity of a nation from the simple as cooking foods to the most complicated use in security bases. Though electric power transmission systems are key infrastructure to a nation, failures followed by blackouts have major consequences for the economy and national security of that nation[13].

The main causes for failures in power transmission could be natural disasters, adverse winds, human or technical failures, labour conflicts, terrorism, acts of war and others[14, 15]. Beside, major power outages can also be caused by combinations of electrical, computer, and human failures and developed in to cascading blackout which affect the customer[14]. Failures or disturbances have starting or initiating event which materialize the disturbance. This event eventually leads to malfunctioning in a power system which may further lead to greater power systems failure and loss of

power access to the subscriber. The technical conditions that may lead to power system failure include: overloads, voltage or frequency outside limits, instability, disconnection of substation or generating plant[14]. In the study of power transmission networks, the structural complexity and the high dependence between components of a power transmission network complicate the study of its behaviour. This interdependence is the main reason of the vulnerability of power transmission network and is translated to the risk of large blackouts.

Vulnerability[1] of the system explains the system's sensitivity to threats or hazards[14]. It is apparent that because of this interdependence, local overloads of lines or local failures of components can generate cascades of current breaks which extremely can cause failure of the whole or part of the network terminologically called blackout. The blackouts can be caused by inefficiency of the power transmission network or by excessive electric current demand from the loads that exceeds the network capacity. It has been shown that there are three main approaches to study the blackout dynamics in the technical and scientific literature studies[16]. The first approach describes the network and between their components interaction in time where the components interaction exhibits equality and inequality constrained algebraic systems of non-linear differential equations. The second approach considers the behaviour of the network at steady state by introducing random fluctuation in the load demand and the third approach considers the power transmission network as an example of complex system whose behaviour depends deeply on its topological properties.

Many researches have been conducted around power transmission networks and the failures arising during the transmission. Power transmission network or power grid consists of generators,transformers, power lines and power stations[2]. The failure in this system means when a disturbance occurs on atleast one of these components or the failure inside a particular component. The failure in the system component can lead to a serious blackout which result huge crises in the society. But most commonly large blackout event or avalanches are not abrupt. Cascading failure is the main mechanism by which large blackouts are likely to happen in such a way that an initial failure in a particular link of the power grid triggers and slack the

[1]The collection of properties of infrastructure system that may weaken or limit its ability to maintain its intended function, or provide its intended services when exposed to threats that originate both within and outside of the boundaries of the system.

real functioning of the rest of the neighbouring links[11, 16–18]. Davide L.Pepnye, in his two folded findings of his work on Topology and cascading outages[18], it has shown that; 1) a failure induced by cascading line outage with high entropy in the interconnection is less likely to happen in irregular grid topology than in regular topology 2)once a cascade line outage is initiated, grids with more entropy or irregular grids are highly fragile leading to breaking apart in to disconnected sub-connections after fewer line failure than regular topologies. Moreover, it was found that in the scenario of cascading failure there could be two types of causes namely deterministic cause and probabilistic cause[19]. Deterministic cause are events in the process of cascading failure that will certainly occur as a result of a single or series of events occur such as overload on certain line due to series outage of components. Probabilistic cause are defined to be the factors directly related to the actual system risk. The probabilistic or stochastic nature of the system behaviour. The component failures, for example Baldick et al.[20] stated that failure of protective relays on its neighbouring lines of the failed one which may cause more lines to trip.

Cascading failure is defined as a sequence of dependent failures of individual components that successively weakens the power system. These failure comprises the physical components, software, procedure, people plus organizations that design,operate and regulate the power system[20]. Cascading outages can be influenced by the details of the system state, such as components out for maintenance and the patterns of power transfer, and the automatic and manual system procedures[17]. Due to complication complete enumeration of all possibilities of cascading is impossible.

An exclusive focus on the causes of the blackout may disregard the global dynamics of complex system in which repeated major disruptions from wide variety of sources is a virtual certainty[21]. The analysis of 15-year time series of North American electric power transmission system blackouts suggested that Self-Organized Criticality(SOC) can govern the complex dynamics of the blackouts[21]. The statistical result of long time correlation and probability density function(PDF) for blackouts size in the North American power grid[1984-1998] was described by SOC. This is consistent with long range time dependencies and PDF for avalanche sizes in running sand pile which is known to be SOC[21].

SOC system is one in which the non-linear dynamics in the presence of perturbations organize the overall average state near, but not at, the state that is marginal to the major disruptions[21, 22]. If the dynamics of the black-

outs are confirmed to have some characteristics of SOC, this would open up possibilities for monitoring statistical precursors of large blackouts or controlling the power system to modify the expected distribution of blackout sizes[22]. The power law tail of outage of transmission lines, as a scale of blackout, has been proved to arise from a process of Self-Organization and cascading failures within the power systems[15]. Conventionally, it was believed that the probability distribution of the blackout to drop exponentially with increasing size of the blackout which resulted in insignificance of large sized blackout. But unlike to the conventional systems, SOC systems which are characterized by spectrum of spatial and temporal scale disruptions, the probability of occurrence of large disruptive events decrease as a power function of the event size[20]. Blackout size is mainly attributed by power shed, energy unserved, customers disconnected, restoration time and number of lines tripped[20].

To understand what measures should be taken in planning management and operation of power systems to avoid disturbances, it is vital to know how often and to what extent disturbances occur[14]. In a reformed electricity market with competition between the utilities, outage analysis is becoming more important. Systems for reporting incidents and disturbances can give increased knowledge on how disturbances arise and how disturbances can be avoided. There are different ways for a failure to smear out through the rest of the network during the blackout event. For example, a transmission line tripping can cause a transient, overloading of other lines, operation or misoperation of relays can contribute to system instabilities. But for the risk of cascading failure, these interactions becomes more severe when the overall system loading increases. And the cascading failure becomes more likely at the critical loading in which the probability of large blackouts and the mean blackout size start to rise quickly. The probability distribution of these blackout sizes has power law dependences [2, 14, 16–18, 21, 23–26].

According to many researches carried such as in Norwegian and North American power grid[21], Swedish[14], Norwegian[2], New Zealand[27] and Chinese[23], the analysis of the failure shows that the size distribution of the event follows power law which implies blackout of all sizes can occur. Example according to J.O.H.Bakke and Kertesz[2], the probability density of the blackout event is proportional to the commutative probability distribution ($\Delta P^{-1.65}$) for the Norwegian power grid and for the North American power grid($\Delta P^{-2.05}$). The significance of power law

in the probability distribution of blackout adds the substantial risk of large blackout near the critical loading[11]. If the blackout cost is proportional to blackout size, the blackout risk(which is the product of blackout size and blackout probability remains constant and resulted in comparable large and small blackout risks[11].

As explained above the probability of occurrence of large disruptive events of SOC-systems decrease as a power function of the event size. But it is not easy task to identify whether a system exhibits SOC type dynamics or not. Nevertheless, the existence of correlations of events over long time scale can be explored to indicate if the system has non-trivial complex dynamics and non-Gaussian properties[25].

Here we will investigate the mechanisms of blackouts statistics in the Norwegian, North American and Ethiopian power grid blackouts. We will emphasise mainly on Scaled window variance(SWV) and rescaled range(RSR) statistics. The cumulative probability distribution for the three power grid systems will also be discussed. Likewise, a squared lattice model will be developed to analyse the statistical and dynamical properties of the blackout event.

Chapter 3

The theoretical analysis of blackout

3.1 Autocorrelation

3.1.1 Scaled Window Variance(SWV) Method

To demonstrate the power loss properties of the practical blackout data for the North American power grid[2] , Norwegian power grid[2] and the Ethiopian power grid[Ethiopian dispatch control center], we will apply the scaled window variance as follows[28]. Each set of data have been considered as a group of time series X_t and the detailed theoretical statistical derivation is referred from[23].

$$X = \{X_t, t = 1, 2, 3, ..., n\} \tag{3.1}$$

The Brownian motion can be constructed from eq.(3.1) as

$$Y = \{Y_t, t = 1, 2, 3, ..., n\} \tag{3.2}$$

Where Y_t is the original time integrated X_t and is given by

$$Y_t = \sum_{i=1}^{t} X_i \tag{3.3}$$

A new series $Y^{(m)}$ is then generated for the series Y and $m = 1, 2, 3, ..., n$. That is,

$$Y^{(m)} = \{Y_u^m, u = 1, 2, 3, ..., n/m\} \tag{3.4}$$

The elements of this series are blocks containing m elements of the initial series Y. Which means

$$Y_u^{(m)} = \{Y_{mu-m+1}, ..., Y_{um}\} \tag{3.5}$$

The standard deviation $\sigma_m^{(u)}$ within each of the n/m blocks and containing m elements is determined as

$$\sigma_m^{(u)} = \sqrt{\sum_{m=1}^{n} \sum_{u=1}^{n/m} \frac{\left((Y_{um-m+1}, ..., Y_{um}) - \mu_m^{(u)}\right)^2}{m}} \tag{3.6}$$

Where $\mu_m^{(u)}$ is the mean of the Brownian motion series of n/m blocks and m elements. After all the average value of the standard deviation $\sigma_m^{(u)}$ over the n/m blocks is calculated as

$$\sigma_m = \frac{\sum_{u=1}^{n/m} \sigma_m^{(u)}}{n/m} \tag{3.7}$$

Thus, the time series X with defined autocorrelation function can be shown that the function σ_m has algebraic tail and scales as power law. That is $\sigma_m \propto m^H$ where H is the Hurst exponent defined earlier. Or

$$log(\sigma_m) = Hlog(m) \tag{3.8}$$

According to [16], for $0.5 < H < 1$, the series X_t has long range time dependent or correlation. And for $0 < H < 0.5$ the series has long time anticorrelations. If $H = 1.0$, the series X_t is deterministic or the output is predictable while it is uncorrelated if $H = 0.5$. Table3.1 shows the autocorrelation analysis of the blackouts of Norway power grid from 1995-2005[2], North America power grid from 1984-2002[2] and Ethiopian power grid from 2005-2012(collected from the Ethiopian dispatch control center), by using SWV method.

Table 3.1: Hurst exponent of blackouts by SWV method

Time series	H
Power lost(MW) of Norwegian	0.93
Power lost(MW) of N.American	1.00
Power lost (MW) of Ethiopian	0.75

The detailed calculation of this table is shown in fig3.1, 3.2 and 3.3 using SWV method. For the North American cases, the result shows $H \approx 1.00$ which roughly shows that there is strong correlations or predictable dependence between successive blackouts. Moreover, the other results indicates that there is still proximity to the long range correlation in the Norwegian as well as the Ethiopian blackouts.

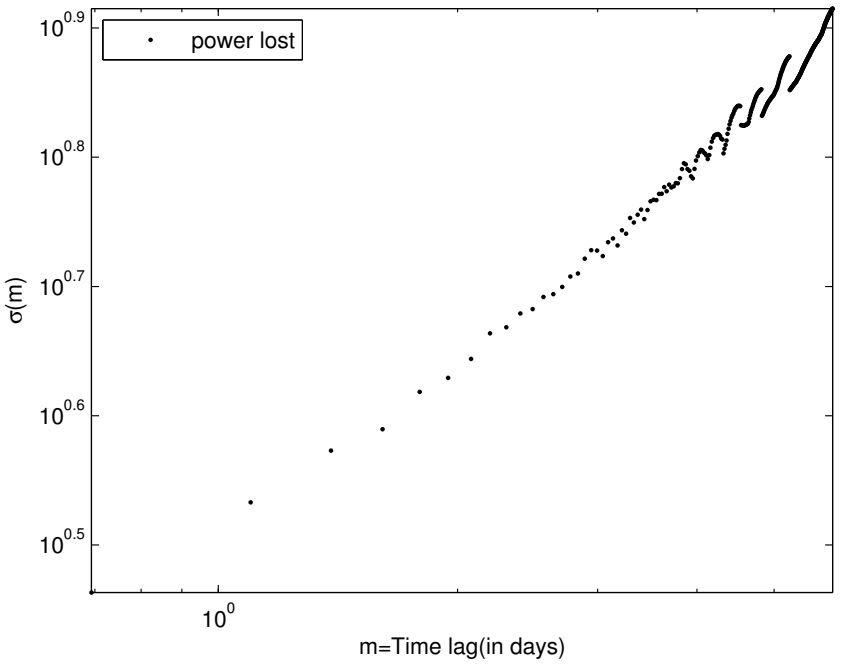

Figure 3.1: Analysis of Norwegian blackout by using SWV method

Figure3.1 shows the log-log plot of the scaled window variance analysis

of the power lost in the Norwegian power grid. The plot represents the standard deviation versus the time delay for the successive time series of blackout events. We found that the standard deviation can be scaled as power law $\sigma_m \propto m^{0.93}$, where m represents the time delay of the successive time series of the blackout event. The number $= 0.93$ is the approximate value of H as already tabulated in table3.1. And since H is less than one but greater than half, it means that there is long range time correlation or dependence between the time series of the blackout events.

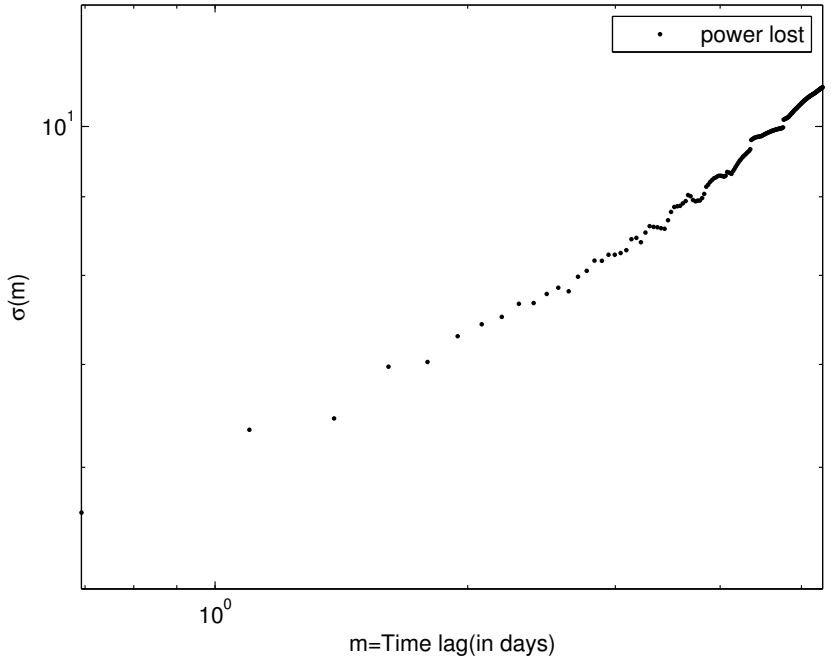

Figure 3.2: Analysis of North American blackout by using SWV method

The above log-log plot in fig3.2 also shows the analysis of power loss for North American power grid in scaled window variance mechanism. Similar to the Norwegian system, the North American system also exhibited power law given by $\sigma_m \propto m^{1.00}$ and the scaling exponent 1.00 is an approximate value for H. However, unlike to the Norwegian case, here $H \approx 1.00$ shows that the time series of blackout is deterministic or the causes of the antecedent events in the time series of the blackout events is sufficiently inevitable.

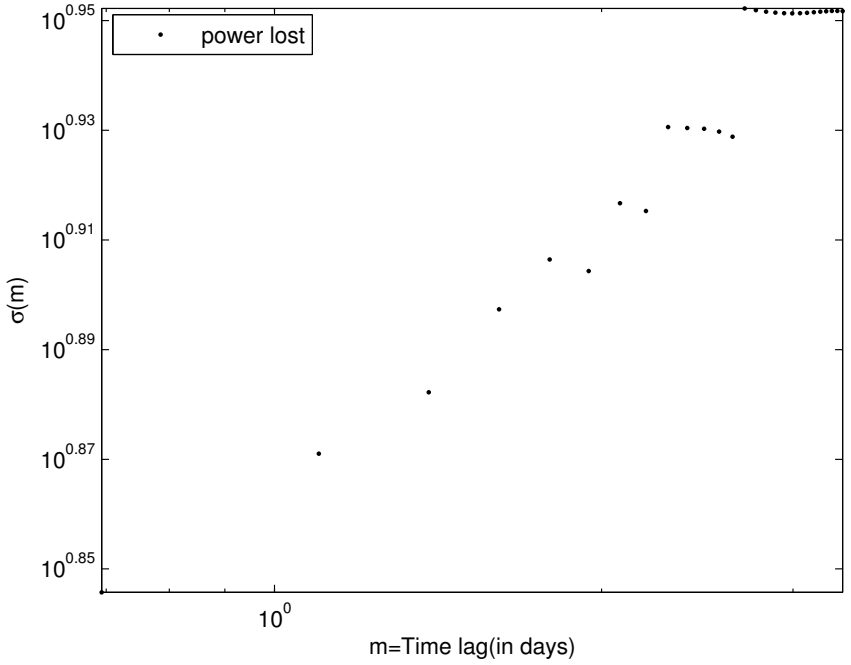

Figure 3.3: Analysis of Ethiopian blackout by using SWV method

Furthermore, fig3.3 shows log-log plot of the scaled window variance analysis of the Ethiopian blackout. The standard deviation is found to be described as $\sigma_m \propto m^{0.75}$ with $H \approx 0.75$. The linear fit for the plot or the slop of this plot represents H and it's value is approximately 0.75. This result is between one and half which signifies the time series of the Ethiopian blackout is also characterized by long-range time correlation.

3.1.2 Rescaled range(RSR) methods

The analysis of the blackout can be alternatively attacked using the rescaled range approach. Similar to the above method a group of time series of the blackout is considered. The blackout is considered as successive time series X_t and Y_t is the Brownian series for it. The statistical analysis is illustrated as follows[23].

$$X = \{X_t; t = 1, 2, 3, ..., n\} \tag{3.9}$$

We can define the average value series of the data as follows with different number of series(τ).

$$\langle X\rangle_\tau = \frac{1}{\tau}\sum_{t=1}^{\tau} X_t, where 1 \leq \tau \leq n \tag{3.10}$$

Then the cumulative deviation of the series is given by

$$Y(t,\tau) = \sum_{n=1}^{t}\{X(n) - \langle X\rangle_\tau\}, where 1 \leq t \leq \tau \tag{3.11}$$

And the range of the data is

$$R(\tau) = max_{1\leq t\leq\tau}Y(t,\tau) - min_{1\leq t\leq\tau}Y(t,\tau) \tag{3.12}$$

And the standard deviation is determined as

$$S(\tau) = \Big\{\frac{1}{\tau}\sum_{t=1}^{\tau}\left(X(t) - \langle X\rangle_\tau\right)^2\Big\}^{\frac{1}{2}} \tag{3.13}$$

The the time series of the blackout event can be scaled as a power law defined

$$R/S \sim (\alpha\tau)^H \tag{3.14}$$

This can be rewritten as

$$log(R/S) \sim Hlog(\tau) + Hlog(\alpha) \tag{3.15}$$

The detailed calculation of the rescaled range analysis for the three electric power systems can be summarized in the following table.

Table 3.2: Hurst exponent of blackouts by RSR method.

Time series	H
Power lost(MW) of Norwegian	0.65
Power lost(MW) of N.American	0.52
Power lost(MW) of Ethiopian	0.70

As we can see in table3.2, the results for H are all larger than half but less than one. This reveals that the results of RSR method is in good agreement with SWV method. They shows similar characteristic properties of the time series of the events in relation to time correlation. The detailed calculation can be graphically shown as in fig3.4, 3.5 and 3.6.

It is worth mentioning that though power generation was started in the late 19th century, yet, the documentation of blackout data in Ethiopia is an old fashion. It is impossible to find well documented and long time recorded data. This is because there is no advanced digital or electronic recording technology to register and keep data long so that further study and amendment on the power system is undertaken. Beside, there is also lack of skilled human power to develop such technology. So, the above analysis of blackout data for Ethiopia is based on limited information. It is clear that a data that is manually recorded and kept in hard file form could result lost and spoils of information. Thus, the results in the statistical analysis of Ethiopian blackout is far from perfection.

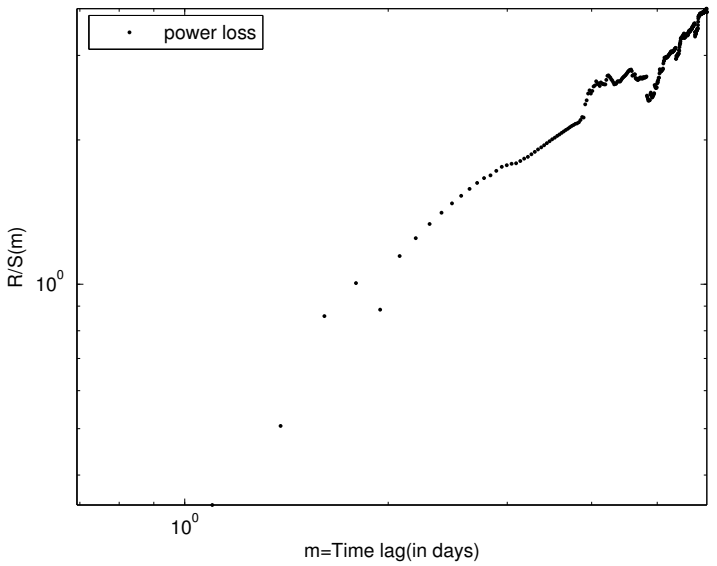

Figure 3.4: Analysis of Norwegian blackout by using RSR method.

Figure3.4 shows log-log plot of the rescaled range method of analysing the blackout. We can see from the plot that the power lost is plotted by

taking time delay between successive time series blackout along the abscissa and the ratio of the range of the time series to the standard deviation of the time series blackout along the ordinate. The linear fit to the plot is implemented to to find power law scaled like $R/S \propto (\alpha\tau)^{0.65}$ where R, S, α and τ are range, standard deviation, scaling constant and average value series(eq.3.10) respectively. The scaling exponent(0.65) is an approximate value for H. Thus, since the value of H in this case is less than one but greater than half, the result is consistent with scaled window variance method. It is found that there is long-range time correlation between successive events of the time series of the Norwegian blackout.

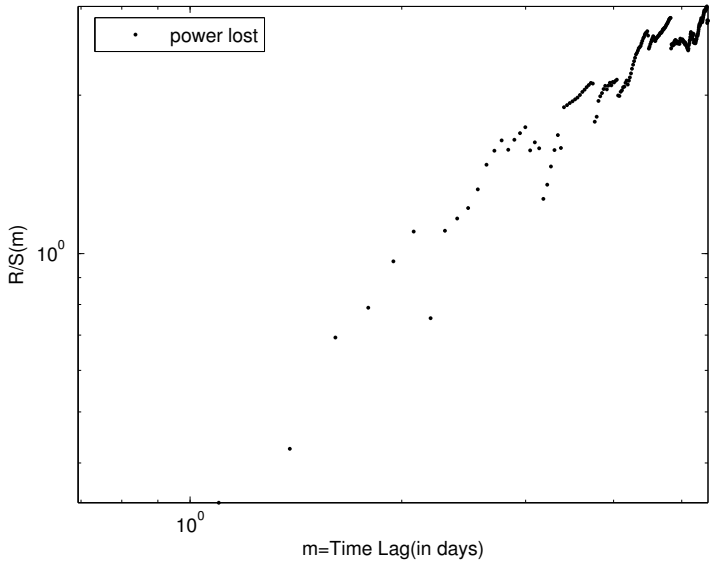

Figure 3.5: Analysis of North American blackout by using RSR method.

This figure3.5 also shows the log-log plot of the rescaled range analysis of the North American blackout. It is found that the the power loss can be possibly scaled by power law described as $R/S \propto (\alpha\tau)^{0.52}$. There is long time range correlation as the value of H is still greater than half though the value in the case of scaled window variance method is approximately 1.00 which showed the dependence on successive events is relatively strong. The reason for the deviation of the numerical result can be the inclusion of large scaled failures caused by hurricanes and ice-storms

in North American data[2] compared to Norwegian and Ethiopian data.

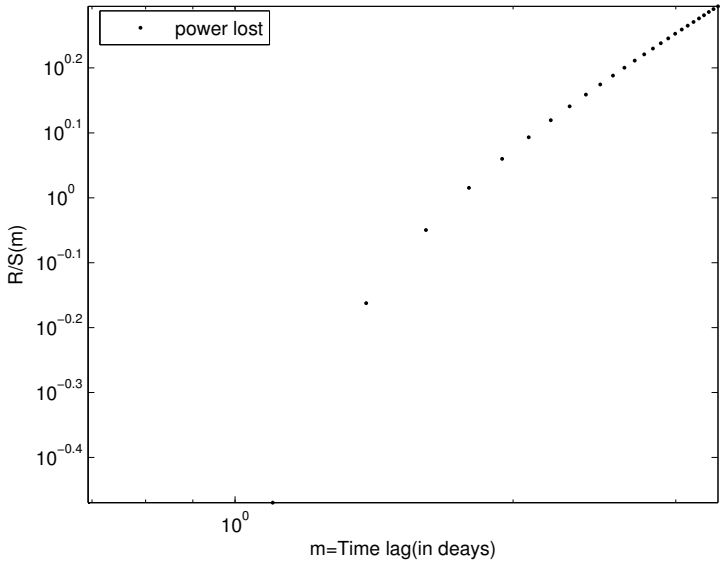

Figure 3.6: Analysis of Ethiopian blackout by using RSR method

Likewise, we can present the rescaled range analysis of the Ethiopian data as shown in figure3.6. The power loss is plotted using log-log mechanism by taking time delay along the abscissa and R/S along the ordinate and it is found that the power loss can be scaled by the power law as $R/S \propto (\alpha\tau)^{0.70}$. This result is similar with the SWV method of analysis for the Ethiopian grid system which shows that there is long time correlation between the blackout events. Thus, it is good to generalize that the power loss could be possibly scaled as power law using both the scaled window variance and rescaled range methods.

Chapter 4

Discussion of Bakke, Hansen and Kertesz model

This model was developed to study the size distribution of blackouts for the Norwegian and North American power grids. The result revealed that the size distribution in both systems follows power law. In addition, the model compares the size distribution in artificial(regular and irregular networks) and real networks.

Statistical analysis of failure in power grid is contingent in energy unserved or power lost. However, though both of these physical quantities leads to power law, in this paper power lost was used to characterize the statistical property of the failure. Because it is believed that this is better quantity compared to energy unserved which can depend on the technical repairing of the failed line by human.The primary goal in this task was to compare the model introduced in this paper with the power loss distribution for the Norwegian, North American[**?**]. It was focused on avalanches triggered by removal of a single node.

The model described the cascade or avalanche effects by considering regular and irregular networks each having the same electrical conductors of the same conductance. First, a current is injected at a random node with another node different from the injection point acting as a current drain. The potential difference that is created between the two nodes helps the determination of each current in the link using kirchhoffs equations[29]. Having the currents i at hand, a breakdown threshold t is assigned to each

link that satisfies linear relationship with the corresponding current.

$$t = (1 + \alpha)i \tag{4.1}$$

where α is a positive number and it represents that each transmission line has been constructed with fixed tolerance α.

Now following similar procedure to random fuse model[30], a link is selected randomly and remove it to initiate the triggering of failure in the network. The currents are then recalculated again. This gives global rearrangement of the network unlike to self-organized criticality[10]. Following this some links will carry currents above the threshold limit. These links are also removed and currents are calculated again. The process of removing will continue as far as there are links in the network which have current values above the boundary or threshold. This removal process models the avalanche effect in the entire network.

To proceed let G_i be the conductance between the source and the sink before the initial random removal of a link and G_f be the conductance at the end of the avalanche process. The difference between these conductance values gives the magnitude of the avalanche size generated during the removal process.

$$\Delta G = G_i - G_f \tag{4.2}$$

Assuming the voltage V between the source and the sink nodes to be fixed during the blackout event, the change in conductance ΔG will be proportional to the power loss.

$$\Delta P = P_i - P_f = V^2 \Delta G \tag{4.3}$$

Where we redefine ΔG for normalization process as

$$\Delta G = \frac{(G_i - G_f)}{G_i} \tag{4.4}$$

The ultimate result found in this study was based on generated ensembles of networks where for each network systematically chosen every link as initiator of the blackout.Two classes of networks have been studied. 1) The Random networks: with exponential degree distribution of $P(k) \propto e^{-0.5k}$ which is the same as for the Norwegian and North American networks. 2) Small-world networks[31] with mean degree 2.67. Mean degree is defined as the average number of edges or links incident to the

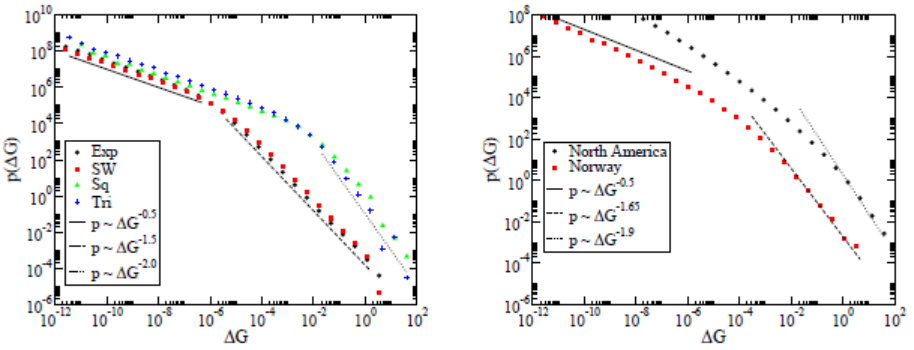

Figure 4.1: Probability density function for the conductance lose[2]

vertexes or nodes[32]. Both classes have mean characteristic length l that scales logarithmically with system size. We can see from the left side of fig4.1 that there are four different plots each of which follows power law. The data for the regular network(triangular and square lattice), moved two orders of magnitude to separate from the irregular lattice(exponential and small-world networks). The right side of the plot indicates the implementation of the model on the Norwegian(1220 nodes) and North American(4941 nodes) power grids. The straight lines shown are the linear fit for the data points and it represents the power law property of the probability density function for the conductance loss.

The simulations have been done with the artificially generated data for network sizes up to 5041 nodes for four different artificial networks applying the conjugate gradient algorithm to solve the kirchhoffs equations[29]. And as it was mentioned above, it has been found from the plot that the probability density of the conductance change for the irregular(random exponential and small-world) and regular lattice follows power law with two different exponents. The one with smaller exponent or small event regime is independent of the network and lattice type, and is approximated by the power function

$$p(\Delta G) \sim \Delta G^{-0.5} \tag{4.5}$$

But the large exponent or large event regime is likely to be dependent on the network type. It is represented by two power law with different exponents. The irregular networks follow power law with exponent of -1.5 ± 0.05 while the regular network is characterized with an exponent of -2.0 ± 0.07.

The simulation has been done for $\alpha = 3.0$. For small values of α, large number of breakdowns resulted in breaking of the system completely with $\Delta G = 1.0$ and the power law tail is destroyed for large ΔG. However, large values of α never change the tail of the distribution. For real power blackout data the largest events recorded affected 5% of the total capacity of the system which reveals that the use α that can't break the system completely($\Delta G < 1$). In addition to this it has been found that the initial current as well as threshold distribution follows power law in both random and small-world networks.

The mean-field estimation of current distribution for the random and exponential network has been found to be

$$P(i) \sim \frac{1}{i} \tag{4.6}$$

The idea here is that when current is injected in to the network at the origin, the cumulative current distribution $P(i)$ is proportional to the average number of links $n(r)$ at a distance r from the origin where $n(r)$ is inversely proportional to $i(r)$. The qualitative analysis of the relation between $n(r)$ and r as well as between $P(i)$ and i is given in the fig4.2

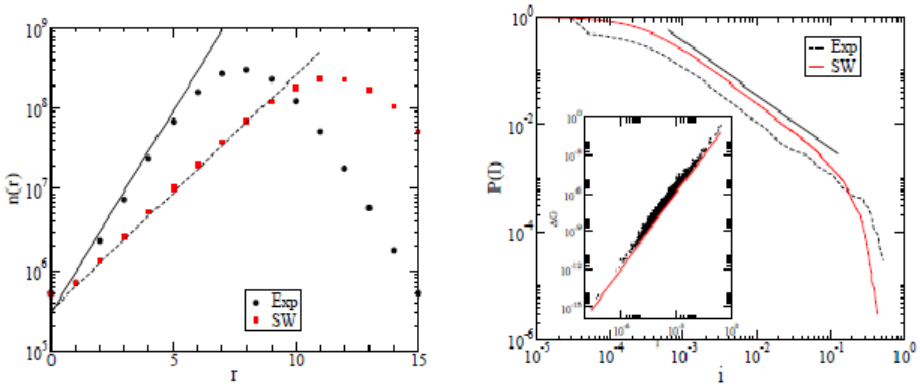

Figure 4.2: a)$n(r)$ versus r for exponential and small-world network. b) $P(i)$ versus i. The inset shows ΔG versus i for $\alpha = 3.0$. The solid line in the inset is i^2. [2]

The left side of fig4.2 represents the average number of neighbours $n(r)$ versus r for the exponential and random networks, and it shows that $n(r)$ is increasing function of r. The straight line represents the increasing slope

of $n(r)$. Moreover, it is worth mentioning that due to finite size for the network, $n(r)$ fall for large value of r. For general cases, $n(r)$ is monotonically increasing function of r if the network considered has infinite size. Similarly the right side of figure4.2 shows the characteristics of cumulative current distribution versus current for 5041 nodes. The distribution function satisfies the relation $P(i) \sim i^{-1}$ which is consistent with the previously theoretically derived result.

The mean-field argument also gives $P(i) \sim i^{-2}$, where $n(r) \sim 1\bar{r}$ for the square and triangular lattice . The derivation of the relation between the conductance loss to the system when a certain bond is removed and the current through that bound is given by

$$\Delta G_k \sim i_k^2 \tag{4.7}$$

where k is the removed bond. From equations (4.6) and (4.7) we could expect the distribution function in terms of conductance loss $p(\Delta G) \sim \Delta G^{-1.5}$ and $p(\Delta G) \sim \Delta G^{-2.0}$ for exponential and random networks, and regular networks respectively which are consistent with the result elaborated in fig4.1. In the end, the results from the simulation have been compared with the analysis of blackouts data from Norwegian main power grid[$\Delta P > 0.1MW$) and the data from the largest blackouts in the North American power grid(with $\Delta P > 10MW$)[2].

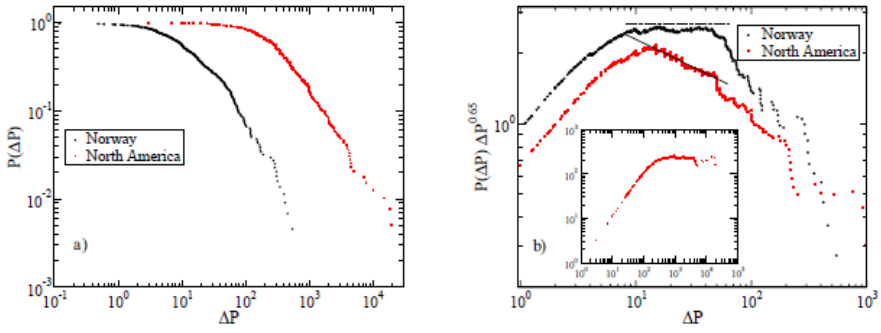

Figure 4.3: a)cumulative distribution $P(\Delta P)$ for power loss in the Norwegian(373 events) and North American(390 events) power grid. b) $P(\Delta P)\Delta P^{0.65}$ for blackout events ΔP for the Norwegian and North American power grid.[2]

In fig4.3, we can see that the cumulative probability reflects the probability to find blackout event larger than or equal to ΔP. This function

was exploited from the real data by ordering in ascending order and plotted event k along the abscissa with $\frac{k}{(N+1)}$ along the ordinate. N is total number of blackout event recorded[2]. Meanwhile, the cumulative probability in the right side of fig4.3 is multiplied by $\Delta P^{0.65}$ after shifting the North American data from the left side of fig4.3 for the sake of simplifying comparison. The ensuing flat plateau in the Norwegian data verifies that the probability density follows power law of the form $p(\Delta P) \sim \Delta P^{-1.65}$ and it falls faster for larger ΔP. But the North American data did not show such plateau rather it gives consistent result with the power law regime corresponding to $p(\Delta P) \sim \Delta P^{-1.9}$. The inset shows $P(\Delta P)\Delta P^{1.05}$ which indicates the probability density to be of the form $p(\Delta) \sim \Delta P^{-2.05}$ for the North American data which is in agreement with -2 exponent for this blackout distribution without cut-off for large ΔP.

In fig4.1, the fitted power laws to the distribution with exponents -1.65 and -1.9 shows the execution of the model on Norwegian and North American power grids[2]. We possibly observe that the artificial data produced by the model are in agreement with real data observed in the Norwegian power grid, however, the observed data for North America are not found to be convincing. Moreover, it can be interestingly observed that the power law for moderately sized blackout data lie in between the results of the model implemented on the irregular networks(exponent -1.5) and regular lattices(exponent -2). But the model doesn't reproduce large-scale blackout distributions for the Norwegian power grid which falls faster than $\Delta P^{-1.65}$ though it is possible to see small-scale regime as observed in fig4.1 of the artificial networks. So, it is possible to infer that the model introduced here is capable of producing some features of the observed blackout distribution quantitatively with reasonable precision.

It can be noted that the inclusion of large events such as snowstorms and hurricanes in the North American data, is the reason for the difference of the distribution for large value of ΔP while the Norwegian data doesn't include these events. The cause of cut-off in the Norwegian data is due to the difference in nature of widespread events like hurricane compared to the power line fault. In addition to this, the reason why the power law or exponent for the Norwegian power grid is close to the irregular networks where this is based on breaking of single link.

Nonetheless, the cause of the difference in the conductance loss distribution from the simulated result of Norwegian and North American power grid is not clear. But looking at more than the degree distribution, it shows

that there are two differences in $n(r)$. The first difference is that for small values of r, $n(r)$ for Norwegian network is closer to the exponential network than North American network. The second is $n(r)$ for Norwegian network is has pronounced peak where as, the North American network is more of plateau compared to Norwegian network. This could elaborate the difference in conductance loss distribution($p(\Delta G)$) observed from the simulation of the networks.

Chapter 5

Square lattice model

Mathematical models developed to describe statistical dynamics in complex systems(example power outages in power grid)are not universally accepted theory but able to reflect some interesting characteristic phenomena. The practically used models are therefore capable of compromising the degree of complication and the expected accuracy of the modelling[33].

Dynamics in complex networks particularly power grid has been modelled using different mechanisms such as cascading model[16, 24], improved OPA model[34], self-organized criticality[10] and so forth which characterizes the power law distribution.

This study will mainly stress on modelling of the transport properties of networks featured by conductance typically the electric power grid. Power grid also called electric power distribution system constitute components like generators, transformers, distribution substations (can be collectively considered as nodes) and the transmission lines. Connectivity in the random networks are statistically homogeneous and the probability of finding highly connected nodes falls exponentially $p(k) \propto e^{-k}$ for $k >$ the mean degree $\langle k \rangle$, where degree k describes the number of links connecting a given node to another node[35, 36]. On the other hand, degree distribution in scale-free(SF) networks follows power law as $p(k) \sim k^{-\gamma}$ where γ represents the scaling exponent[24]. It can be noticed that it is unlikely to have high degree probability in the random network. In other words, for the same number of nodes and edges, the probability of high degree nodes is less in random networks than scale free networks[35]. According to Watts and Strogatz (1998), regular networks such as power grid is char-

acterized by small world property locally with high degree of clustering and globally small characteristic length[35]. Clustering coefficient is defined as the magnitude of the connectivity extent to which neighbours of a certain node connected to it are also connected to each other. characteristic length is also defined as the number of edges in the shortest possible path connecting two nodes averaged over all the nodes of the network. Sparsely distributed power grids have less mean degree such as Norway compared to North America's power grid which is densely scattered[35]. So, it is not difficult to guess that Ethiopian power grids have very small mean degree(not researched) because the available power supply in the country is very limited.

The failure distribution for Norwegian and North American has already been studied and showed that the size of the failure distribution follows power law[2]. This study of size distribution was based on power loss on the Norwegian and North American power grid. The statistics of failures can possibly depend not only on power loss but also on energy unserved. However, energy unserved is not preferable quantity to characterize the size of failure as it depends on human(technicians) time taken to restore the transmission line from malfunctioning.

We will now present a model which is similar to the model in chapter four to describe the cascading effects quantified by power loss. We will consider $L \times L$ squared lattice(see fig5.1) where each nodes situated at the lattice are connected by transmission lines of fixed tolerance[5]. Biperiodic boundary condition is imposed to incorporate large bonds of the system for simulation. Following the same procedure as the the previous model in chapter four, we first injected a current randomly to a selected node with another node different from the first node considered as current drain. The network is assumed to have electrical conductors of the same conductance. The potential difference created between the two nodes can be solved by kirchhoffs equation to find the current in each link using conjugate gradient method[29]. Steepest descent method[37] is the simplest and efficient method in conjugate gradient technique to handle particular systems of linear equations(kirchhoffs equation in our case) which is the same as successive one dimensional minimization of the function constructed by a series of voltage vectors along the direction of local gradient[29]. Following the determination of the currents in each link, a breakdown threshold t given by eq(4.1), is assigned to each link.

The network can now be perturbed by systematically choosing a link

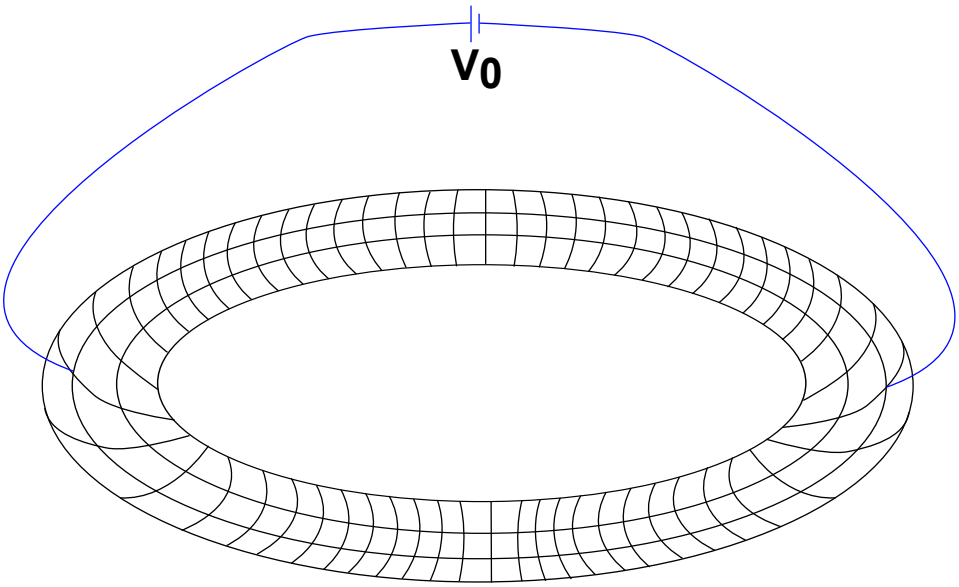

Figure 5.1: Square lattice network

and removing it so that current redistribution through out the intact lattice will occur. Then the new current in each link is recalculated and found that the current is globally redistributed unlike to self-organized criticality[10] which prohibits local rearrangement for certain type of failure. This time more or less there is contingency in the transmission lines since they are forced to carry an extra or deficit of the load due to the removal of the link. Therefore, some links will carry a current larger than their threshold capacity and then these links are removed from the system. The currents in the still intact part of the network are again calculated. The process of removing links with current higher than the limiting amount continue until all links will have a current less than the boundary.

The difference of the conductance between source and sink before initial random removal(G_i) and the conductance after the avalanche is finished(G_f) measures the size of the avalanche generated during the removal process(eq(4.2)). Then the power loss due to this avalanche is determined by eq(4.5). Now we will plot the conductance change versus probability density function using the data generated by our model. It is good to note that we use log-log mechanism to plot the following figures.

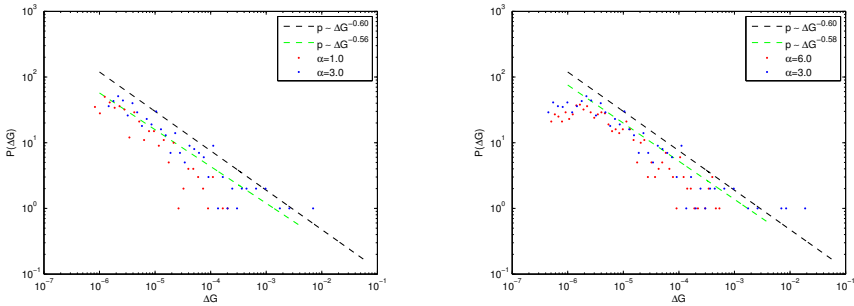

(a) **(b)**

.

Figure 5.2: a) Illustration of 180×180 probability density function of conductance loss for $\alpha = 1.0$ and $\alpha = 3.0$. b) Illustration of 180×180 probability density function of conductance loss for different value of $\alpha = 3.0$ and $\alpha = 6.0$

Fig5.2 shows the probability density of conductance change ΔG for 180×180 square lattice. As shown in fig.5.2a), we observe that the conductance change follows power law characterized by $p(\Delta G) \propto \Delta G^{-0.56}$ for $\alpha = 1.0$ and $p(\Delta G) \propto \Delta G^{-0.60}$ for $\alpha = 3.0$. We also found that the probability density of the conductance change follows power law described as $p(\Delta G) \propto \Delta G^{-0.58}$ for $\alpha = 6.0$(fig.5.2b). The scaling exponent of the conductance change or head of the power law distribution decrease from -0.56 to -0.60 when the value of alpha increases from $\alpha = 1.0$ to $\alpha = 3.0$. But when α increase from 3.0 to 6.0, the scaling exponent falls from -0.60 to -0.58 without significant change on the tail of the power law distribution. This tells us the robustness of transmission lines towards failure increases with its tolerance capacity up to specific value of α(which is approximately 3.0 for this case study) and head of the density distribution remains almost constant above this value. On the contrary, the tail of the power law for the conductance change disappears for smaller value of $\alpha(\alpha < 3.0)$. This is because when the tolerance value for the electrical conductor is small, they are easily exposed to breakdown which leads to large sized blackout events as we have already observed in our simulation. So, for small value of α, the tail of the probability density does not behave like power law distribution.

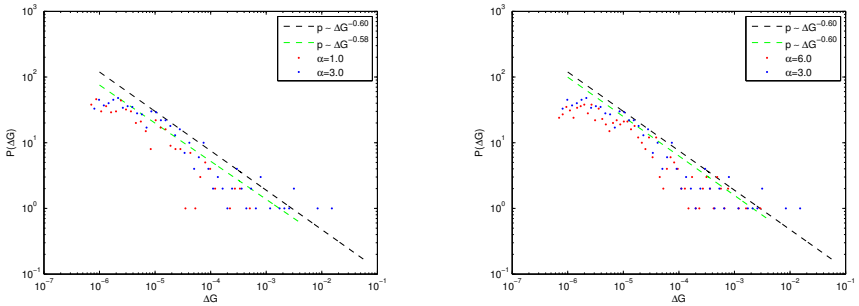

(a) **(b)**

Figure 5.3: a) Illustration of 160×160 probability density function of conductance loss for $\alpha = 1.0$ and $\alpha = 3.0$. b) Illustration of 160×160 probability density function of conductance loss for different $\alpha = 3.0$(blue data points) and $\alpha = 6.0$

In fig5.3, we are able to see similar properties as in fig.5.2. The probability density function of the conductance loss follows power law given by $p(\Delta G) \propto \Delta G^{-0.58}$ and $p(\Delta G) \propto \Delta G^{-0.60}$ respectively for $\alpha = 1.0$ and $\alpha = 3.0$ as shown in fig.5.3a. The probability density function of the conductance loss also follows power law expressed as $p(\Delta G) \propto \Delta G^{-0.60}$ for $\alpha = 6.0$(fig.5.3b). In the same argument as before, the scaling exponent of the power law for the conductance change decrease from -0.58(for $\alpha = 1.0$) to -0.60(for $\alpha = 3.0$). But unlike to 180×180 lattice size, increasing α further never changed the exponent of the conductance change as shown in fig.5.3b. We can infer from this that for 160×160 lattice size, the scaling exponent of the conductance change depends on α up to certain value which is 3.0 and remains constant for larger value of α. On the other hand, comparing the scaling exponent of conductance change in fig.5.2a and fig.5.3a for case $\alpha = 1.0$ as well as in fig.5.2b and fig.5.3b for case $\alpha = 6.0$, it reveals that the exponent decreases from -0.56 to -0.58 and from -0.58 to -0.60 respectively when the lattice size decreases from 180 to 160. But the exponent remains constant for $\alpha = 3.0$ which is -0.60. Thus, the scaling of the power law for conductance change also depends on lattice size when $\alpha \neq 3.0$. But for $\alpha = 3.0$, it is constant for lattice size 180 and 160.

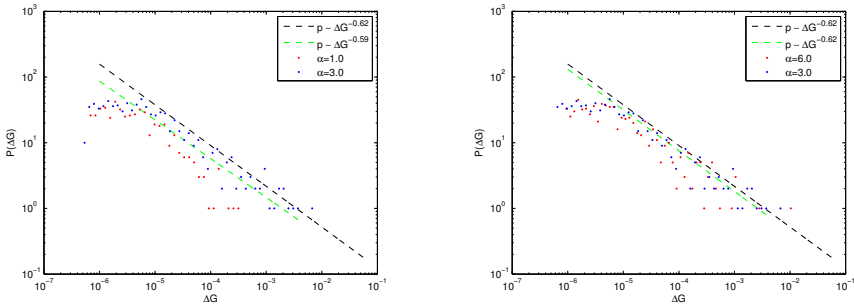

(a) **(b)**

.

Figure 5.4: a) Illustration of 140×140 probability density function of conductance loss for $\alpha = 1.0$ and $\alpha = 3.0$. b) Illustration of 140×140 probability density function of conductance loss for different values of $\alpha = 3.0$ and $\alpha = 6.0$

Fig5.4 is also the probability density function for the squared lattice with 140×140. We found that the exponent of the conductance change specially its head is the same for $\alpha = 3.0$ and $\alpha = 6.0$ which is given by the relation $p(\Delta G) \propto \Delta G^{-0.62}$ (see fig.5.4b). But as shown in fig.5.4a, the probability density drops from $p(\Delta G) \propto \Delta G^{-0.59}$ to $p(\Delta G) \propto \Delta G^{-0.62}$ when α increased from 1.0 to 3.0 while it remains constant when α increased to 6.0. This also concludes that for a square lattice of size $L = 140$, the robustness of the electrical conducting lines depends on the tolerance up to specific value which is numerically 3.0. Beside to this, for a fixed value of $\alpha(\ 0 < \alpha < 3.0)$, fig.5.3a and fig.5.4a shows the exponent of the power law for conductance change decreases from -0.58 to -0.59, and in fig.5.3b and fig.5.4b, the exponent drops from -0.60 to -0.62 for $\alpha \geq 3.0$.

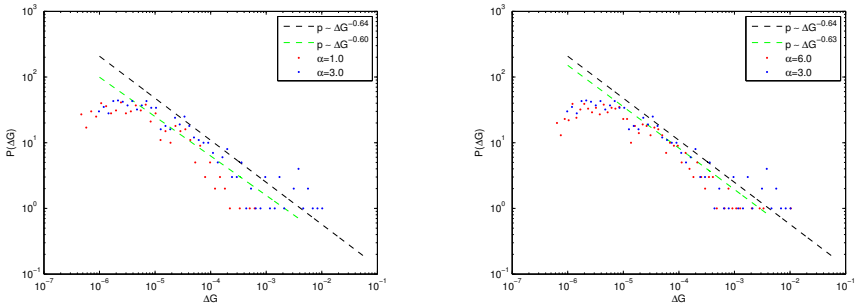

(a) **(b)**

.

Figure 5.5: a) Illustration of 120×120 probability density function of conductance loss for $\alpha = 1.0$ and $\alpha = 3.0$. b) Illustration of 120×120 probability density function of conductance loss for different values of $\alpha = 3.0$ and $\alpha = 6.0$

The same characteristics of the power law is observed for the square lattice 120×120 of fig.5.5. The relation $p(\Delta G) \propto \Delta G^{-0.64}$ and $p(\Delta G) \propto \Delta G^{-0.60}$ describes the probability density of the conductance change for $\alpha = 3.0$ and $\alpha = 1.0$ respectively(fig.5.5a). And the probability density of the conductance change for $\alpha = 6.0$ is found to be $p(\Delta G) \propto \Delta G^{-0.63}$. We can see from the probability density expressions that still the conductance change depends on the value of α for $\alpha < 3.0$ though there is slight deviation for $\alpha > 3.0$. Furthermore, comparing to fig.5.4, the power of conductance change decreases from -0.59 to -0.60 for $\alpha = 1.0$ and from -0.62 to -0.64 for $\alpha = 3.0$(see fig.5.4a and 5.5a). So, for fixed α, again we see that the strength of the conductance change dependence on the lattice size decreases when the lattice size is decreased from $L = 140$ to $L = 120$.

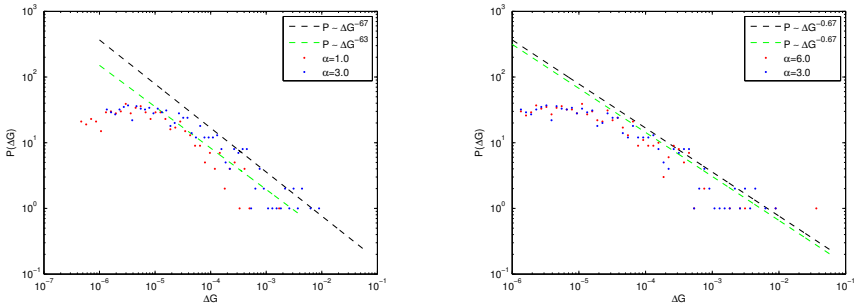

(a) **(b)**

.

Figure 5.6: a) Illustration of 100×100 probability density function of conductance loss for $\alpha = 1.0$ and $\alpha = 3.0$. b) Illustration of 100×100 probability density function of conductance loss for different values of $\alpha = 3.0$ and $\alpha = 6.0$

Fig.5.6 shows the probability density function of conductance change for different values of α. In fig.5.6a, we see that the probability density of the conductance change is described by $p(\Delta G) \propto \Delta G^{-0.63}$ for $\alpha = 1.0$ and $p(\Delta G) \propto \Delta G^{-0.67}$ for $\alpha = 3.0$. Moreover, $p(\Delta G) \propto \Delta G^{-0.67}$ describes the probability density for $\alpha = 6.0$(see fig.5.6b). From the plots we can deduce that $L = 100$ also display the same properties as the earlier lattice sizes. Beside, the exponent of the conductance change has also dropped compared to the conductance change for lattice size $L = 120$.

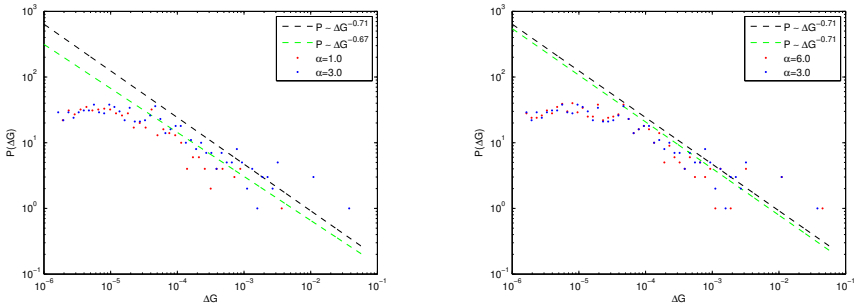

(a) **(b)**

.

Figure 5.7: a) Illustration of 80×80 probability density function of conductance loss for $\alpha = 1.0$ and $\alpha = 3.0$. b) Illustration of 80×80 probability density function of conductance loss for different values of $\alpha = 3.0$ and $\alpha = 6.0$

Figures 5.7a and b, represents the probability density described by $p(\Delta G) \propto \Delta G^{-0.67}$ and $p(\Delta G) \propto \Delta G^{-0.71}$ respectively for $\alpha = 1.0$ and $\alpha = 3.0/\alpha = 6.0$. The result shows the exponent of the probability density of the conductance change decreases from -0.67 to -0.71 when α increased from 1.0 to 3.0 and remained constant when α increased to 6.0. Thus, for fixed value of lattice size $L = 80$, the conductance change depends on tolerance up to specific value(i.e $\alpha = 3.0$] but the scaling exponent for the conductance change remains the same when α increased further. And when we look at the dependence of conductance change on lattice size under constant α of fig.5.7 relative to fig.5.6, the scaling exponent declined from -0.63 to -0.67 for $\alpha = 1.0$(see fig.5.6a and 5.7a), and from -0.67 to -0.71 for $\alpha = 3.0, 6.0$(see fig.5.6b and 5.7b).

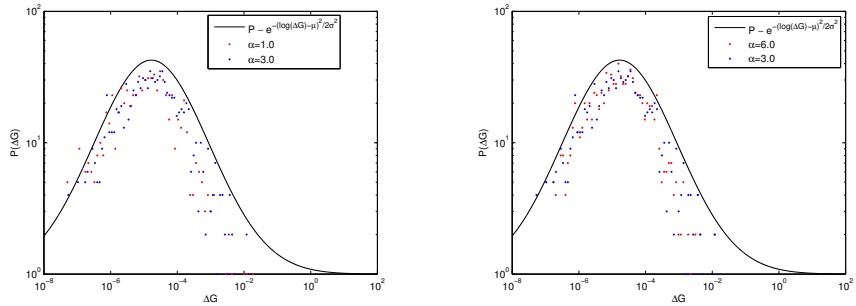

(a) **(b)**

.

Figure 5.8: a) Illustration of 60×60 probability density function of conductance loss for $\alpha = 1.0$ and $\alpha = 3.0$. b) Illustration of 60×60 probability density function of conductance loss for different values of $\alpha = 3.0$ and $\alpha = 6.0$

Fig.5.8 shows the probability density of the conductance change for the squared lattice sized 60×60. Unlike the previous properties, the probability density of the conductance change follows Gaussian distribution of the form $p(\Delta G) \propto e^{\frac{-(log(\Delta G)-\mu)^2}{2\sigma^2}}$, where $\mu = -11.0$ is the mean of the distribution and $\sigma^2 \approx 2.80$ is the variance of the distribution. It is worth mentioning that the negative value of mean indicates the conductance value between the source and the drain of the system of the conducting lines before an initial removal of the link is less than the conductance value after the end of the avalanche. We also found that the probability density of conductance change is similar for all all values of α.

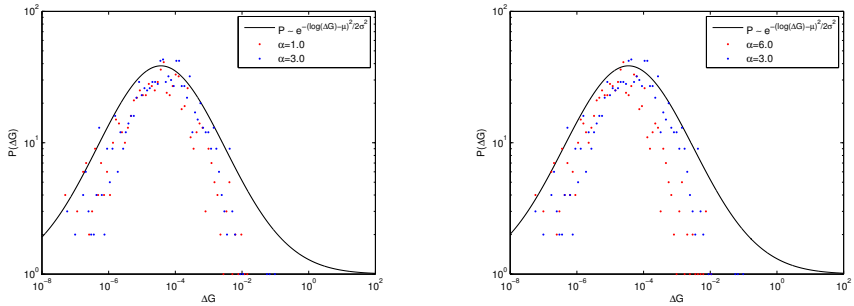

(a) **(b)**

.

Figure 5.9: a) Illustration of 40×40 probability density function of conductance loss for $\alpha = 1.0$ and $\alpha = 3.0$. b) Illustration of 40×40 probability density function of conductance loss for different values of $\alpha = 3.0$ and $\alpha = 6.0$

For small values of the lattice size(40×40) or for the squared lattice containing small number of nodes the probability density function of the conductance change follows Gaussian distribution given by $p(\Delta G) \propto e^{\frac{-(log(\Delta G)-\mu)^2}{2\sigma^2}}$, with a negative mean value($\mu \approx -10.0$) and variance($\sigma^2 \approx 3.0$). The negative value of mean tells us that the conductance change between the source and the sink of the network before the initial removal of the link is less than the conductance change after the avalanche is finished. From fig.5.9, we can see that the probability density is similar for all values of α which implies that the for small value of lattice size, probability density of the conductance change behaves like Gaussian and is independent of the tolerance value.

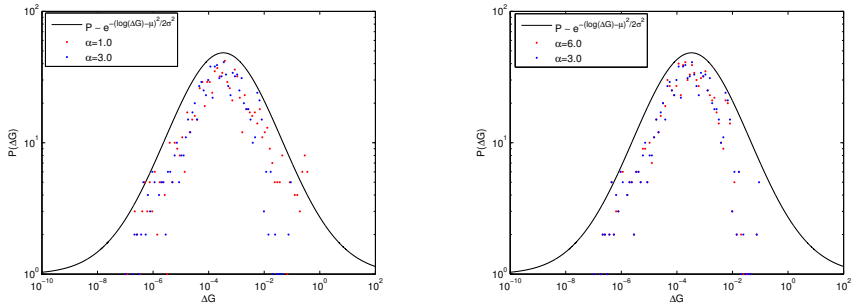

(a) **(b)**

.

Figure 5.10: a) Illustration of 20×20 probability density function of conductance loss for $\alpha = 1.0$ and $\alpha = 3.0$. b) Illustration of 20×20 probability density function of conductance loss for different values of $\alpha = 3.0$ and $\alpha = 6.0$

Referring to this figure5.10, the probability density of the conductance change fallows Gaussian distribution like for the lattice sizes $L = 60$ and $L = 40$. The plot shows that for all values of $\alpha > 1.0$, the probability density describing the conductance change is similar and defined by the relation $p(\Delta G) \propto e^{\frac{-(log(\Delta G)-\mu)^2}{2\sigma^2}}$, where μ is the mean with a value of approximately -8.0 and variance $\sigma^2 \approx 3.2$. The negative value of the mean signifies the same argument as earlier Gaussian distributions. The only difference observed is that the right tail of the previous Gaussian distributions(fig.5.8 and 5.9) is short while for $L = 20$ or fig.5.10, the right and left tails are almost similar and relatively fatter. The cause of shorter tails in fig.5.8 and 5.9 can be be argued that for relatively small lattice sizes($L < 80$), at the beginning of the removal process of modelling the avalanche effects, the removal of the links in the first few iterations can't lead to blackout event. On the contrary at the end of the removal process due to threshold, produces relatively successive blackout events which resulted longer right tail in the Gaussian distribution.

Now we will see the qualitative properties of the practical blackout data's for the North American power grid, Norwegian power grid and Ethiopian (collected from the Ethiopian dispatch control center of the power distribution). As it was mentioned in chapter three, the Ethiopian data are mainly from 2005-2012 but all the events that happened between this period was

not recorded and that it is not inclusive. So, the data is small enough due to the fact that EEPCO(Ethiopian Electric Power Corporation) has no modern technology to record data rather they were using the traditional way of recording blackout data which could result loss of important data used for further study purpose. Due to this reason, it was difficult to find long time recorded data for studying the over all properties of blackout event in Ethiopia. However, we tried to investigate the statistical analysis with the data at hand though it is far from perfection. As per the technician's description, the main reasons for Ethiopian power failures are human operation, earth fault, heavy raining and lightning. Thus, only small scale blackouts occur while the North American power grid also incorporate failures due to hurricanes, and snowstorms that makes loss of power in large scale. Moreover, power service in Ethiopia is very limited because power infrastructure in Ethiopia is very limited as it is developing country. Therefore, limitation of the power coverage has its own impact in statistical study of the blackout event. This is because, the data collected is not large enough to make concluding analytical or statistical results describing the real power system dynamical property.

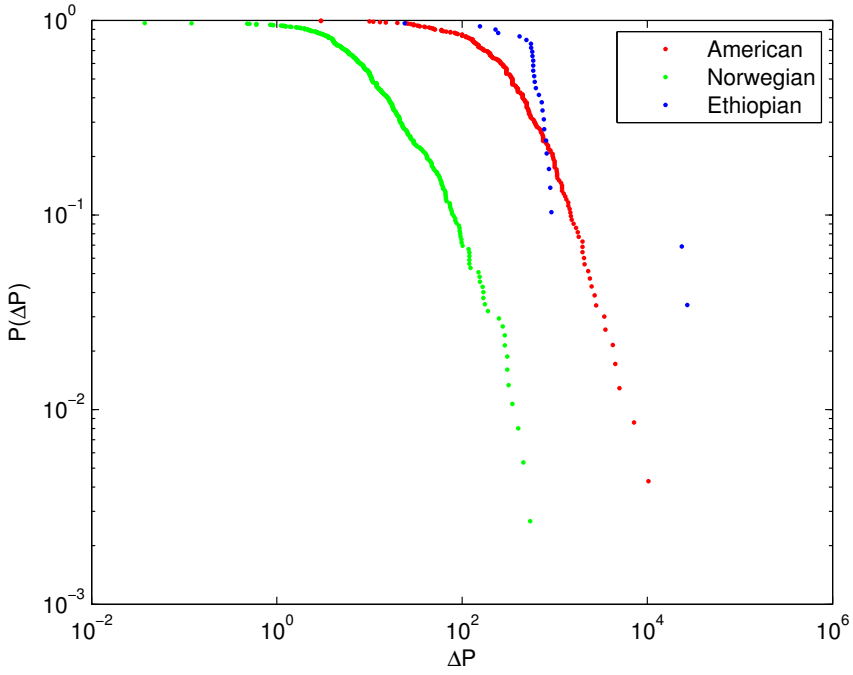

Figure 5.11: Cummulative distribution $P(\Delta P)$ for blackout events in the American(232events), Norwegian(373 events) and Ethiopian(28 events)

Figure5.11 shows the cumulative probability $P(\Delta P)$ giving the probability to find an event larger or equal to the change in power lost(ΔP). This function(ΔP) is extracted from the corresponding data by ordering them in descending order and then plotting using log-log mechanism with the event β(which represent ΔP) along the abscissa and $\frac{\beta}{(N+1)}$(representing $P(\Delta P)$) along the ordinate. N represents the total number of events in the corresponding country. The result showed that all the data follows power law, and with the available data, it shows that Norwegian data has larger scaling exponent than North American as well as the Ethiopian data while North American data has slightly larger exponent and in a short range regime falls below Ethiopian data.

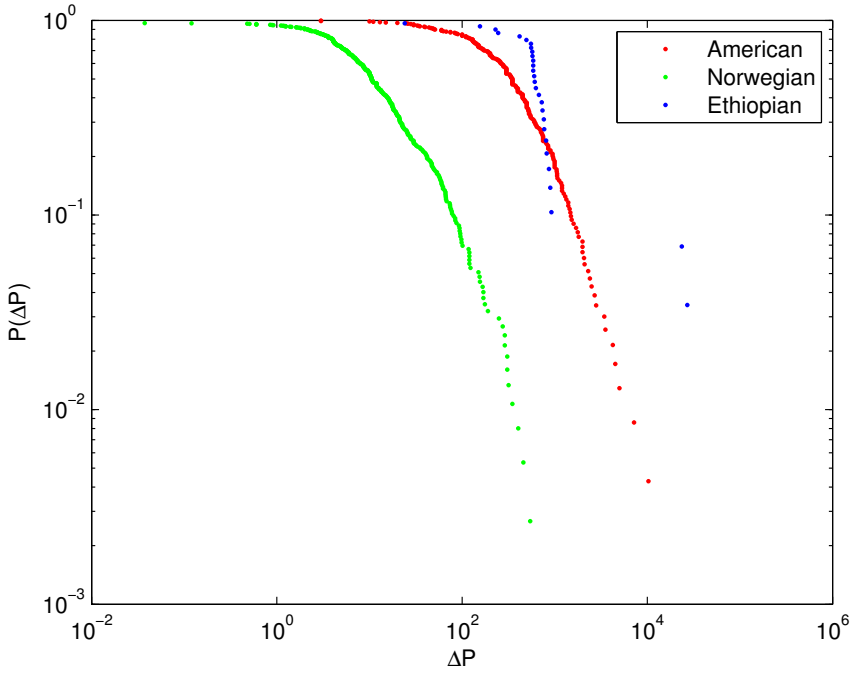

Figure 5.12: Cummulative distribution $P(\Delta P)$ for blackout events in the American(232events), Norwegian(373 events) and Ethiopian(28 events)

Figure5.12 represents the cumulative probability of finding an event larger or equal to power lost(ΔP). But unlike to the above, here the function (ΔP) is extracted from the data by ordering them in ascending order and plotting using log-log approach with the event β along the abscissa and $1 - \frac{\beta}{(N+1)}$ along the ordinate. As we can see from the plot, we found similar properties as the preceding figure.

Chapter 6

Conclusion

Blackout is considered as unexpected phenomena in electrical power grids because it happens without warning which makes effect analysis and modelling to be relatively complicated. The prominent objective of this paper is to study the characteristics of the size distribution of failures in the Norwegian, North American and Ethiopian power grids. Moreover, blackout event is modelled by the squared lattice network. The numerical analysis of squared lattice network is conducted to show the statistical properties of failures prone in a specified network.

The theoretical statistical analysis of the blackout events occurred in the Norwegian, North American and Ethiopian power grids is examined by mechanisms of SWV and RSR. The correlation or dependence between successive events of the blackout is determined using the above two methods. On the other hand, the model developed here is to understand the probability distribution of the blackout event in a squared lattice network. The avalanche in this network is triggered by systematic removal of a single node from the link, where the links are constructed from conducting lines of the same conductance.

The SWV and RSR analysis of time series of blackout events recorded from the Norwegian, North American and Ethiopian power grid shows that the event can be scaled by power law and the scaling exponent gives the Hurst coefficient of the time series of blackouts. The Hurst coefficient quantifies the degree of correlation between time series of successive events. We found that in both cases(SWV and RSR), the value of Hurst coefficient for the Norwegian data is $0.50 < H < 1.00$. This indicates that in the Nor-

wegian power grid, there is long range time dependence between blackout events which means high value of the blackout event in the time series will be probably followed by another high event and its converse. The North American data also showed that the value of the Hurst exponent is between 0.50 and 1.00 and hence long-range time correlation between the events. The SWV and RSR analysis for Ethiopian data are also in good agreement giving the Hurst exponent to be 0.75 and 0.70 which is in the range for long range time dependence between the blackout events. But it is hard to believe the analysis in the case of Ethiopian power grid because the empirical data given is too small. Thus, further study is recommended to widen the coverage of multiple blackout events for sake of perfection.

The statistical analysis of computer generated data in the squared lattice model is also presented. we found that the probability density function for the conductance change follows power law and the scaling exponent of the power law represents the dependence of the conductance change or power loss on the tolerance of the conducting line or the size of the lattice. For a fixed lattice size($180 \leq L \leq 80$), we show similar characteristics. The scaling exponent for the conductance change decrease when α increased from 1.0 to 3.0 but increasing α to 6.0 does not change the tail of the power law though there is slight deviation on the head of the distribution. Similarly, for fixed $\alpha(1.0 \leq \alpha \leq 3.0$ and $3.0 \leq \alpha \leq 6.0)$, the scaling exponent increases when the lattice size increased from $L = 80$ to $L = 180$. However, the probability density function for the conductance change behaves Gaussian distribution for the lattice size less than 80. Close to $L = 80$, the left tail of the distribution is shorter compared the right which is also slightly fatter where as, for $L = 20$, the tails of the distribution are equivalent.

We also analysed the probability distribution or cumulative distribution for the empirical data of blackout event for the Norwegian, North American and Ethiopian power grids. The distribution follows power law for all the data and it shows that all the distribution function($P(\Delta P)$) falls faster for large value of ΔP.

Bibliography

[1] U.S. Canada Power System Outage Task Force. *Final Report on the August 14, 2003 Blackout in the United States and Canada*. U.S Secretary of Energy and Minister of Natural Resources Canada, 2004.

[2] A. Hansen J.O.H.Bakke and Kertesz. Failures and avalanches in complex networks. *Journal of Europhysics. Lett*, 76(4), 2006.

[3] Cutler J.cleveland. *Encyclopedia of Energy*. Elsevier Academic Press, 2004.

[4] G. N. Tiwari and R. K. Mishra. *Advanced Renewable Energy Sources*. RSC, 2012.

[5] J. A. Alves-Gomes. The evolution of electroreception and bioelectrogenesis in teleost fish: a phylogenetic perspectiv. *Journal of Fish Biology*, 2001.

[6] Moller Peter and Bernd Kramer. Electrocomunication in teleost fishes: Behavior and experiment. *American Institute of Biological Science*, 41(11):794–6[794], 1991.

[7] Gordon Keith Chalmers. The lodestone and the understanding of matter in seventeeth century england. *The University of Chicago Press*, 4 (1):75–95, 1937.

[8] Hubregt J. Visser. *Array and Phased Array Antenna Basics*. John Wiley and Sons, Ltd, 2005.

[9] Matthew H. Brown and Richard P. Sedano. *Electricity Transmission: A Primer*. NCSLS, 2004.

[10] Xingyong Zhao, Xiubin Zhang, and Bin He. Study on self organized criticality of china power grid blackouts. *Energy Conversion and Management*, 50(3), 2009.

[11] Dusko P. Nedic, Ian Dobson, Daniel S. Kirschen, Benjamin A. Carreras, and Vickie E. Lynch. Criticality in a cascading failure blackout model. *International Journal of Electrical Power and Energy Systems*, 28(9), 2006.

[12] de Arcangelis, L., Redner, S., and Herrmann, H.J. A random fuse model for breaking processes. *J. Physique Lett.*, 46(13), 1985.

[13] D.E. Newman, B.A. Carreras, V.E. Lynch, and I. Dobson. Exploring complex systems aspects of blackout risk and mitigation. 60(1), 2011.

[14] . Holmgren and S. Molin. Using disturbance data to assess vulnerability of electric power delivery systems. 12(4), 2006.

[15] Duan Xianzhong and Su Sheng. Self-organized criticality in time series of power systems fault, its mechanism, and potential application. *Power Systems, IEEE Transactions on*, 25(4), 2010.

[16] A. Farina, A. Graziano, F. Mariani, and F. Zirilli. Probabilistic analysis of failures in power transmission networks and phase transitions: Study case of a high-voltage power transmission network. *Journal of Optimization Theory and Applications*, 139(1), 2008.

[17] M. Vaiman, K. Bell, Y. Chen, B. Chowdhury, I. Dobson, P. Hines, M. Papic, S. Miller, and P. Zhang. Risk assessment of cascading outages: Methodologies and challenges. *Power Systems, IEEE Transactions on*, 27(2), 2012.

[18] DavidL. Pepyne. Topology and cascading line outages in power grids. *Journal of Systems Science and Systems Engineering*, 16(2), 2007.

[19] Bei Gou and Weibiao Wu. Is the prediction of power system blackouts possible? In *Power and Energy Society General Meeting - Conversion and Delivery of Electrical Energy in the 21st Century, 2008 IEEE*, 2008.

[20] R. Baldick, B. Chowdhury, I. Dobson, Zhaoyang Dong, Bei Gou, D. Hawkins, H. Huang, Manho Joung, D. Kirschen, Fangxing Li, Juan Li, Zuyi Li, Chen-Ching Liu, L. Mili, S. Miller, R. Podmore, K. Schneider, Kai Sun, D. Wang, Zhigang Wu, Pei Zhang, Wenjie Zhang, and Xiaoping Zhang. Initial review of methods for cascading failure analysis in electric power transmission systems ieee pes cams task force on understanding, prediction, mitigation and restoration of cascading failures. In *Power and Energy Society General Meeting - Conversion and Delivery of Electrical Energy in the 21st Century, 2008 IEEE*, pages 1–8, 2008.

[21] B.A. Carreras, D.E. Newman, I. Dobson, and A.B. Poole. Evidence for self-organized criticality in a time series of electric power system blackouts. *Circuits and Systems I: Regular Papers, IEEE Transactions on*, 51(9), 2004.

[22] B.A. Carreras, V.E. Lynch, D.E. Newman, and I. Dobson. Blackout mitigation assessment in power transmission systems. In *System Sciences, 2003. Proceedings of the 36th Annual Hawaii International Conference on*, pages 10 pp.–, 2003.

[23] Xiaofeng Weng, Yiguang Hong, Ancheng Xue, and Shengwei Mei. Failure analysis on china power grid based on power law. *Journal of Control Theory and Applications*, 4(3), 2006.

[24] Rong LiLi Wang Jian-wei. Effect attack on scale-free networks due to cascading failures. *Chines Physics Lett*, 25(10), 2008.

[25] B.A. Carreras, D.E. Newman, I. Dobson, and A. B. Poole. Initial evidence for self-organized criticality in electric power system blackouts. In *System Sciences, 2000. Proceedings of the 33rd Annual Hawaii International Conference on*, pages 6 pp.–, 2000.

[26] Benjamin A Carreras, Vickie E Lynch, ML Sachtjen, Ian Dobson, and David E Newman. Modeling blackout dynamics in power transmission networks with simple structure. 2001.

[27] Graeme Ancell, Conrad Edwards, and Vladimir Krichtal. Is a large scale blackout of the new zealand power system inevitable. In *Electricity Engineers Association 2005 Conference Implementing New Zealands Energy Options, Aukland, New Zealand*, 2005.

[28] Michael J. Cannon, Donald B. Percival, David C. Caccia, Gary M. Raymond, and James B. Bassingthwaighte. Evaluating scaled windowed variance methods for estimating the hurst coefficient of time series. *Physica A: Statistical Mechanics and its Applications*, 241 (34), 1997.

[29] Ghassan George Batrouni and Alex Hansen. Fourier acceleration of iterative processes in disordered systems. *Journal of Statistical Physics*, 52(3-4), 1988.

[30] Paolo Crucitti, Vito Latora, and Massimo Marchiori. A topological analysis of the italian electric power grid. *Physica A: Statistical Mechanics and its Applications*, 338(12), 2004.

[31] M.E.J. Newman and D.J. Watts. Renormalization group analysis of the small-world network model. *Physics Letters A*, 263(46), 1999.

[32] M. Rosas-Casals. Power grids as complex networks: Topology and fragility. In *Complexity in Engineering, 2010. COMPENG '10.*, pages 21–26, 2010.

[33] Janusz W. Bialek Jan Machowski and James R. Bumby. *Power System Dynamics*. John Wiley and Sons, Ltd, 2008.

[34] Shengyu Wu Shengwei Mei F. H., Xuemin Zhang and Gang Wang. An improved opa model and blackout risk assessment. *IEEE TRANSACTION ON POWER SYSTEMS*, 24(2), 2009.

[35] Reka Albert, Istvan Albert, and Gary L. Nakarado. Structural vulnerability of the north american power grid. *Phys. Rev. E*, 69, 2004.

[36] Strogatez Steven H Watts, Duncan J. Collective daynamics of small-world networks. *letters to Nature*, 393, 1998.

[37] Gene H. Golub. Charles F. Van Loan. *Matrix Computations*. The Johns Hopkins University Press, 1983.

Appendix

The following are the empirical data obtained from the three different power grid systems.

The Norwegian blackout data(power loss in megawatt) from 1995-2005

Event no.	P.loss(MW)	Event no.	P.loss(MW)	Event no.	P.loss(MW)	Event no.	P.loss(MW)
1	4.000147	47	67	93	3	139	3.89625
2	4.000154	48	18	94	10.94118	140	0.6
3	6.7	49	9.975	95	10.37778	141	120
4	13.4	50	96	96	26.02597	142	123.0769
5	16.4	51	28	97	6.8	143	4.191
6	4.026316	52	46.90909	98	37.6	144	4.448
7	98.67568	53	27.6	99	60	145	9.886479
8	48.92308	54	0	100	13.8	146	12.03246
9	31.5	55	25.2	101	21.2	147	15.345
10	4.2	56	38.29091	102	9.6	148	84.135
11	4.2	57	18	103	21.21951	149	41.6702
12	2.4	58	40.90909	104	55.55556	150	7.47
13	9.12	59	0	105	60	151	47.1
14	0	60	17.72727	106	16.089	152	40.592
15	7	61	0	107	3.002264	153	21.33
16	12	62	35.58621	108	3.20151	154	68.075
17	21.81818	63	7.5	109	10.58333	155	74.06217
18	0	64	10.38462	110	10.72571	156	1.816957
19	0	65	10.28571	111	9.6225	157	5.811818
20	23.07692	66	13.38462	112	10.58824	158	6.06359
21	24	67	56.30769	113	35.05667	159	27.99
22	27.6	68	61.15385	114	47.08333	160	14.1
23	19.2	69	15.92308	115	10.90941	161	1.638571
24	17.53846	70	5.15625	116	4.502264	162	77.21825
25	20.90909	71	7.4	117	26.07488	163	19.3045
26	7.090909	72	2.142857	118	17.53412	164	30.33575
27	2.64	73	5.46	119	9.05	165	101.1193
28	12	74	1.976471	120	11.91632	166	57.91375
29	3.6	75	0.6	121	7.410353	167	25.73925
30	9.6	76	17.62222	122	22.73455	168	74.4605
31	9.6	77	4.08	123	13.75	169	1.160727
32	9	78	4.1	124	10.58824	170	2.89443
33	6	79	4.0995	125	460	171	5.88507
34	3.169811	80	22.5	126	4.379486	172	3.163448
35	6	81	22.5	127	2.314118	173	8.394
36	1.2	82	22.5	128	3.643548	174	64.99964
37	8	83	4.05	129	1.383636	175	23.21167
38	1.111111	84	4.05	130	21	176	4.352727
39	3.846154	85	2	131	26.58	177	21.024
40	6.666667	86	12.6	132	78	178	10
41	5.5	87	12.6	133	33.06	179	20
42	8.571429	88	12.6	134	0.506941	180	6
43	15.56962	89	7.004348	135	4.04465	181	8.468571
44	0	90	5.7	136	0.12	182	2.8
45	19.43662	91	5.7	137	13.30955	183	18.1813
46	1.44	92	5.7	138	6.510067	184	11.892

The Norwegian blackout data(power loss in megawatt) from 1995-2005

Event no.	P.loss(MW)	Event no.	P.loss(MW)	Event no.	P.loss(MW)	Event no.	P.loss(MW)
185	2.649231	231	66.24	277	12.77419	323	4.545
186	2.748	232	12	278	1.25	324	4.7
187	3.9	233	3.603604	279	10.16949	325	5.04
188	5.079474	234	2.2965	280	7.5	326	4.911667
189	8.02	235	3.636363	281	4.956522	327	5.331475
190	6.356	236	3.6	282	17.5	328	190
191	66.66	237	10.4745	283	2.93617	329	8.571429
192	15.016	238	7.044	284	57.3913	330	10.06
193	51.3624	239	0	285	16.98113	331	4.873594
194	8.744	240	170	286	8.25	332	75.86441
195	1.7175	241	3.5	287	0	333	7.8
196	14.52727	242	87	288	2	334	2.74
197	28.86	243	10.54545	289	9.086118	335	150
198	10.276	244	10.8	290	2.553191	336	7.5
199	5.07	245	10.23529	291	6	337	19.73684
200	6.726486	246	9	292	50	338	3.306122
201	3.524	247	156	293	2.769231	339	3.333333
202	8.568	248	1.615385	294	317.5714	340	10
203	1.8	249	2.307692	295	307.5556	341	10.02
204	5.664706	250	1.25	296	81	342	62.34375
205	0.846207	251	15.5	297	20	343	62.34375
206	274.464	252	42	298	0.0375	344	10
207	176.1525	253	18.4	299	4.35	345	32.12927
208	92.72727	254	6.521739	300	12	346	117.6
209	8.625	255	84.54545	301	25.5	347	59.01639
210	25	256	403.6364	302	307.7143	348	7.121739
211	6.580645	257	2.25	303	0.917143	349	4.2
212	16.95882	258	3.625	304	0	350	4.071429
213	98.19512	259	7.267606	305	6	351	5.4
214	2.198473	260	4.178571	306	30	352	16.57895
215	17.805	261	6.428571	307	30	353	21.315
216	23.7	262	3.333333	308	250	354	12.015
217	43.4625	263	7.272727	309	36.92308	355	4.285714
218	120	264	5.207547	310	18	356	0.889362
219	10.8	265	16.28	311	21.66667	357	53.55
220	154.6154	266	66.10169	312	544.8	358	16.2
221	94.2	267	53.57143	313	288.7619	359	120
222	67.2973	268	15	314	348.6774	360	10.56
223	0.48	269	2.142857	315	167	361	16.851
224	170	270	6.163636	316	48	362	7.963636
225	120	271	45.24	317	4	363	12
226	19.475	272	7.8	318	30	364	14.07158
227	18.82154	273	16.5	319	39.89189	365	8.688889
228	14.38364	274	8.790698	320	73.33333	366	4.909091
229	12.265	275	13.375	321	95.45455	367	0
230	20.675	276	45.76271	322	42	368	11.15143

The Norwegian blackout data(power loss in megawatt) from 1995-2005

Event no.	P.loss(MW)
369	4.77333333
370	2
371	290
372	93.75
373	0.6

North American Blackout data(power loss in megawatt) from 1984-2002

Event no.	P.loss(MW)	Event no.	P.loss(MW)	Event no.	P.loss(MW)	Event no.	P.loss(MW)
1	335	45	4500	89	3525	133	850
2	383	46	20	90	280	134	900
3	75	47	300	91	28	135	90
4	550	48	34	92	30	136	640
5	586	49	170	93	110	137	60
6	380	50	1600	94	250	138	300
7	85	51	25	95	145	139	1400
8	200	52	162	96	1170	140	150
9	739	53	1477	97	1816	141	300
10	850	54	30	98	1000	142	900
11	350	55	1048	99	150	143	125
12	530	56	520	100	400	144	1700
13	514	57	637	101	545	145	2000
14	1200	58	3440	102	618	146	110
15	60	59	1116	103	450	147	425
16	230	60	290	104	750	148	470
17	730	61	2070	105	138	149	698
18	75	62	450	106	480	150	1000
19	300	63	819	107	972	151	130
20	300	64	280	108	500	152	44
21	1000	65	520	109	155	153	960
22	11	66	2500	110	218	154	100
23	713	67	1200	111	950	155	300
24	1400	68	258	112	130	156	40
25	713	69	240	113	750	157	1525
26	677	70	60	114	500	158	46
27	30	71	118	115	350	159	143
28	205	72	168	116	200	160	200
29	4235	73	150	117	350	161	500
30	2800	74	88	118	500	162	50
31	400	75	480	119	200	163	130
32	300	76	325	120	26	164	294
33	200	77	300	121	110	165	138
34	300	78	550	122	350	166	175
35	530	79	564	123	400	167	35
36	132	80	100	124	750	168	325
37	10	81	150	125	10280	169	190
38	400	82	3	126	2300	170	450
39	133	83	373	127	260	171	130
40	350	84	3	128	450	172	13
41	350	85	350	129	1500	173	160
42	1000	86	800	130	150	174	1775
43	5000	87	257	131	600	175	1300
44	121	88	2000	132	2000	176	530

North American Blackout data(power loss in megawatt) from 1984-2002

Event no.	P.loss(MW)	Event no.	P.loss(MW)
177	460	221	51
178	450	222	1060
179	500	223	270
180	430	224	67.6
181	2700	225	1060
182	116	226	400
183	1340	227	212
184	340	228	250
185	1250	229	7200
186	750	230	2400
187	600	231	63
188	350	232	950
189	350		
190	620		
191	100		
192	500		
193	390		
194	1050		
195	185		
196	134		
197	144		
198	49		
199	168		
200	263		
201	1200		
202	340		
203	190		
204	196		
205	274		
206	39		
207	2100		
208	213		
209	334		
210	1450		
211	210		
212	32.8		
213	48		
214	83		
215	278		
216	15		
217	240		
218	100		
219	848		
220	1071		

Ethiopian blackout data(power loss in megawat from 2005-2012

Event no.	p.loss(MW)
1	26999.141
2	23555.789
3	921
4	896.83002
5	868
6	818.40002
7	809.85999
8	771
9	765
10	738
11	726.40002
12	675
13	625.40002
14	608
15	601.20001
16	586.40002
17	585.90002
18	585.5
19	576
20	571.59998
21	558
22	553.20001
23	494.10001
24	417
25	245.5
26	230
27	156
28	24